Microfluidic platform for integrated compartmentalization of single zoospores, germination and measurement of protrusive force generated by germ tubes

Yiling Sun,[a,c] Ayelen Tayagui,[b,c] Ashley Garrill[b,†], and Volker Nock[a,c,†]

[a] Department of Electrical and Computer Engineering, University of Canterbury, Christchurch, New Zealand.
[b] School of Biological Sciences, University of Canterbury, Christchurch, New Zealand.
[c] The MacDiarmid Institute for Advanced Materials and Nanotechnology, Wellington, New Zealand
[†]Correspondence to Volker Nock, volker.nock@canterbury.ac.nz or Ashley Garrill, ashley.garrill@canterbury.ac.nz

List of contents:

Part I: Methods

Device Fabrication

Both gas and fluidic layer of the platform were fabricated by PDMS casting from photoresist masters, as shown in Fig. S1.

For the gas layer photoresist master, standard photolithography processing was utilized. A 4 inch chrome-on-glass photomask (Nanofilm, USA) with the gas layer pattern was firstly drawn using L-EDIT (v2019.2, MentorGraphics, USA) and then prepared using a pattern generator (μPG101, Heidelberg Instruments, Germany). In parallel, a 4 inch silicon wafer (Prime grade, single-side polish, WaferPro, USA) was pre-cleaned by dehydration for 2 hours in a 185 °C oven and oxygen plasma (100 W, 10 min, Tergeo, PIE Scientific, USA). It was then coated with negative dry-film photoresist (SUEX 100, thickness 100 μm, DJ Microlaminates, USA) and soft-baked for 15 min at 65 °C on a hotplate (Cimarec+, ThermoFisher, NZ). The photoresist was exposed using a mask aligner (MA-6, SUSS MicroTec, Germany) with an exposure dose of 900 mJ/cm² in low vacuum contact-mode with a short wavelength filter (PL-360, Chroma, USA), and post-exposure baked using a ramped process of 65 °C for 5 min and 95 °C for 10 min on a hotplate (HS40, Torrey Pines Scientific, USA). The master mold of the gas layer was completed by development in Propylene glycol methyl ether acetate (PGMEA, Sigma-Aldrich, NZ), rinsing with IPA and drying by N_2, followed by a hard-bake at 150 °C for 1 hour on a hotplate (HS40, Torrey Pines Scientific, USA).

The two-layer photoresist master of the fluidic layer was fabricated by replica-molding off a two-layer resist master, where the second layer provided the vertical spacer between the top of micropillar and channel lid. Two masks were designed using L-EDIT (v2019.2, MentorGraphics, USA). The first layer mask contained the channel outlines, inlets and outlets, while the second layer mask contained the same features with the addition of measurement pillars. As described above, two 4 inch chrome-on-glass photomasks (Nanofilm, USA) were then prepared using a tabletop micro pattern generator (μPG101, Heidelberg Instruments). The photomasks were again chrome wet-etched in the in-house-made etchant, containing 16.5 g ceric ammonium sulphate and 4.3 ml perchloric acid in 100 ml DI water, and rinsed with DI water, followed by development in resist developer (AZ MIF326, Merck, Germany). In parallel, a dry-film negative photoresist (ADEX05, thickness 5 μm, DJ Microlaminates, USA) was laminated on a pre-cleaned 4 inch silicon wafer and exposed using the first layer photomask at exposure dose of 170 mJ/cm² in low vacuum contact-mode on the MA-6 aligner with the same short wavelength filter. After a ramped post-exposure bake, the wafer was developed in cyclohexanone for 5 min, rinsed with IPA and dried using N_2. Then, a positive photoresist (AZ 40XT, MicroChemicals, Germany) was spin-coated onto the first layer at a speed of 2000 rpm, edge-bead removed and soft-baked for 3 min at 126 °C on a hotplate. The wafer was exposed again with the second layer photomask at an exposure dose of 250 mJ/cm² and post-exposure baked at 105 °C for 80 sec on a hotplate. The master mold for fluidic layer was completed by development in AZ 326MIF for 3 min, rinsing with DI water, and drying with N_2.

The photoresist masters of the gas and fluidic layers were treated with Trichloro(1H,1H,2H,2H-perfluorooctyl) (TFOCS, Sigma-Aldrich, NZ) in a vacuum desiccator for 30 min before PDMS casting. Pre-mixed and degassed polydimethylsiloxane (PDMS, 10:1 w/w, Sylgard 184, Electropar, NZ) was poured onto the molds, degassed again, and baked at 80 °C for 2 hours on a hotplate. After curing,

the PDMS chips were carefully peeled off from the masters. Meanwhile, the elastic membrane was produced on another 4 inch silicon wafer. In brief, a pre-cleaned wafer was treated by vapour-coating with TFOCS in a desiccator for 30 min. Pre-mixed and degassed PDMS (10:1 w/w) was then spin-coated onto the wafer at 3000 rpm for 30 s on a spin-coater (WS-650, Laurell, USA), and cured by baking on a hotplate for 2 hours at 80 °C. Examples of fabricated photoresist masters and corresponding PDMS replicas are shown in Figs. S2 and S3.

After manually punching the gas inlet port using a 1 mm diameter biopsy punch (ProSciTech, Australia), the gas layer was bonded to the PDMS membrane, still attached to the silicon wafer, by oxygen plasma (100 W, 30 s, Tergeo, PIE Scientific, USA) and heated for 2 hours at 80 °C on a hotplate. Following this, the bonded structure, including the PDMS membrane, was carefully peeled off from wafer and the zoospore and media inlets/outlets ports manually punched using the same size biopsy punch. Finally, the fluidic layer and membrane with gas layer were both plasma-treated again (O_2, 100 W, 30 s, Tergeo, PIE Scientific, USA), visually aligned and bonded together in a custom-built desktop aligner.[1] In order to prevent valve sticking, vacuum pressure was applied to the sealed gas layer via a vacuum pump (Anest Iwata Sparmax, Taiwan) during the alignment, bonding and baking processes via Tefzel tubing and a 9-inlet manifold (both IDEX Health Science, USA). This vacuum was held throughout the whole process and prevented the valve membranes from contacting their respective valve seats while the surface of both layers was still oxygen-activated, as shown in Fig. S4.

To aid with vacuum application, and thus prevent valve membrane sticking, micro-posts had to be added into the gas inlets. Without these, vacuum application led to the collapse of the membrane during alignment and thus blockage of the interface between the manually-cored inlet holes and gas channels, as shown in Fig. S5. Layers were aligned and brought into contact with the fluidic layer sitting on the XY stage under the microscope while the vacuum was continuously applied to the gas layer. The two layers were irreversibly bonded after being baked for 2 hours at 80 °C on a hotplate with the vacuum on. To complete the assembly process, deionized water (DI) water was injected into the fluidic layer through the zoospore inlet after baking and before the vacuum application was stopped. After this, the valve membrane was relaxed onto the valve seat. This was necessary to prevent the PDMS membranes from attaching to their respective valve seats, as shown in Fig. S6(a – c). Without DI water, valves were observed to initially open, but then permanently bond to the valve seat (Fig. S6(d & e)).

Following assembly, devices were stored filled with DI water in the fluidic layer until experiments were performed. The latter was necessary to prevent the collapse of sensing pillars towards the side walls of the channels during drying out of the fluidic chips. Should dry storage be required, this could be eliminated by the use of supercritical CO_2 drying.[2]

For device visualization, the gas layer and fluidic layer were filled with epoxy dyes.[3] In brief, up to 2 mg of the desired Sudan dye (Sigma-Aldrich, Sudan I (yellow, 103624), Sudan II (orange, 199656), Sudan Blue II (306436), Sudan IV (solvent red, 198102), Sudan Red 7B (fat red, 201618), and Sudan Black B (199664)) per milliliter of toluene was poured into a glass vial (Arthur Holmes, New Zealand). The vial was then manually shaken to ensure that the Sudan dye was thoroughly mixed in the toluene. Following this, 250 µL of UV-curable Norland Optical Adhesive (NOA 72, Norland Products) was added to the vial and manually shaken until the NOA was thoroughly mixed. The vials were then left in a fume hood at room temperature until

all the toluene evaporated, which took ≈7 days mL^{-1} of toluene (in a small vial). Once prepared, the epoxy dyes were kept in a fridge and brought to room temperature prior to use. For loading and curing of the dyes, the microfluidic chips were placed under vacuum in a desiccator for ≈2 h to enable passive filling of the epoxy dye.[4] After removing the microfluidic chip from the desiccator, a pipette was used to place a small droplet of the desired epoxy dye on the inlets of the chip. Following this, the microfluidic chip was left on a flat bench until all the microchannels were entirely filled. Once the microfluidic chips were filled, the epoxy dye was exposed to UV light at a wavelength of 365 nm using an OmniCure S2000 Spot UV Curing System (Excelitas).

Zoospore Production

As shown in Fig. S7(a), a nappy liner (Asaleo Care, Australia) was cut slightly smaller than the diameter of a Petrie dish, boiled 3 times for 10 min each in distilled water, and autoclaved. It was then placed carefully on peptone yeast glucose (PYG) agar (Thermo Fisher, NZ) in a Petri dish (containing [in% w/v] peptone [0.125], yeast extract [0.125], glucose [0.3], and agar [2]). Six inoculum plugs from a fresh culture growing edge of *A. bisexualis* were cut on a 45° angle to reduce the amount of media transferred across. The inoculation plugs were evenly spread around the plate on the nappy liner. After incubation at 26 °C for 24 hours, the nappy liner with the colony growing on it was peeled off from the PYG agar, and placed aseptically into a 250 ml flask with 100 ml autoclaved PYG broth inside (containing [in% w/v] peptone [0.125], yeast extract [0.125] and glucose [0.3]). Following gentle swirling on an orbital shaker at 150 rpm for 24 hours at 26 °C in the dark (Fig. S7(b)), the PYG broth in the flask was exchanged with mineral salt solution (containing 5 mM KNO_3, 10 mM $Ca(NO_3)_2$, 4 mM $MgSO_4$, 20 mM $FeSO_4$ and 20 mM di-sodium Ethylene diamine tetra acetic acid (EDTA, Sigma Aldrich, NZ) five times in the first hour. Between each change, the flask was returned to the orbital shaker at 26 °C and shaken at 150 rpm. The sixth time, solution exchange was implemented after 1 hour of swirling on orbital shaker at 150 rpm, 26 °C, after which the flask was again replaced on the orbital shaker and left overnight. The next day the contents in the flask were poured through two layers of sterile Kimwipes (Thermo Fisher, NZ) into a sterile flask, as shown in Fig. S7(c), and put on vortex for 10 s to collect the encysted zoospores in solution. Finally, the supernatant of the solution was removed, and collected zoospores were re-suspended in mineral salt solution and stored in a 4 °C fridge. Before experiments, the zoospore solution was mixed with fresh PYG broth (1:1 v/v) and incubated at 26 °C for 2 hours to induce zoospores to germinate and increase in size.

Zoospore Characterisation

The size distribution of encysted zoospores was determined using tuneable resistive pulse sensing (TRPS)[4,5] with a qMicro machine (IZON Science, NZ). *Achlya* zoospores were obtained as per the protocol described above. The zoospore solution was mixed with filtered 5% phosphate-buffered saline (PBS) solution (1:1 v/v). Measurements were made using an MP50 micropore filter (ID B04732, IZON Science, NZ). To calibrate the qMicro machine, 20.06 µm plain polystyrene particles (CP20M, IZON Science, NZ) were made up at a concentration of 0.31% solids, corresponding to a dilution of 700:1 in filtered 5% PBS solution. After a series of calibration runs of

the qMicro machine to stabilise the measurement current, a maximum pressure of 3 cm H_2O and a voltage of -1.60 V were established for the measurements. A volume of 0.5 mL of the zoospore solution was added to the machine for the TRPS measurements. Results were analysed and plotted, as shown in Fig. S8, as particle count versus particle diameter in the qMicro software suite (Control Suite V3.3, IZON Science, NZ).

Zoospore germination

After distributing the zoospore solution into several centrifuge tubes, these were centrifuged at 800 rpm for 10 min at 20 °C, and the supernatant of the solution was carefully removed. The zoospores in the bottom of the tubes were re-suspended in the mineral salts solution, and stored at 4 °C until use. Germination of zoospores was observed after mixing of the produced zoospore solution with PYG broth (1:1 v/v) and incubation at 26 °C for 2 hours. Compared with initially produced zoospores, shown in Fig. S7(d), the zoospores grew larger and started putting out a germling after 2 hours of culture (Fig. S6(e&f)). In order to also demonstrate the germination of *A. bisexualis* zoospores on the PDMS device, a series of zoospores in PYG broth media (1:1 v/v) were introduced. After 2 hours of culture on the platform, a number of zoospores were observed starting to germinate. These germlings grew robustly and branched after 7 hours, as shown in Fig. S7(g), indicating good compatibility with the PDMS material.

Experimental setup and force sensing

Zoospore solution was introduced to the device with a syringe pump (NE-300, New Era Pump Systems, USA) via the zoospore inlet, while media and valve pressure were supplied using a microfluidic flow controller (OB1 Mk3+, Elveflow, France) coupled with a microfluidic flow sensor (MFS1, Elveflow, France). A syringe pump was used for the zoospore solution because it did not require a flow sensor for flow rate feedback. The MFS1 sensor providing feedback to the microfluidic flow controller has an internal diameter of ~25 µm, which may make it prone to blockages when used with the zoospores. Individual control of normally-closed microvalves was achieved using a microfluidic Quake valve controller (MUX Quake Valve, Elveflow, France), which was introduced between the pressure controller OB1 and gas inlet ports to operate individual microvalves in three states, including fully open (negative pressure = -1.0 bar), partially closed (pressure = 0 bar), and completely closed (positive pressure = +1.0 bar). Blunt-end 90 degree bent needle tips (18 gauge), silicone tube adapters and were utilized to connect inlets and outlets ports to the other equipment to optimize available space between each port. The media inlet was connected to the flow sensor, then a 5 mL reservoir (Eppendorf, NZ) was filled with media and the pressure controller OB1 used to provide constant and continuous flow of media during zoospore culture. Experiments were observed and recorded using an inverted microscope (TS100, Nikon, Japan) and an attached digital colour camera (MQ013CG-E2, Ximea, Germany) connected to a PC running digital acquisition software (CAMTool, Ximea, Germany).

The performance of the separately-controlled membrane valves and hydrodynamic traps was tested using 20 µm diameter polystyrene microspheres (Polybead, Polysciences, USA) suspended in DI water coloured with food dye (Hansell's, NZ) to simulate and visualize zoospore media. Media diffusion into closed

measurement channels over time was characterised by analysing recorded colour images of the channels in ImageJ. Colour images were imported, split into red, green and blue channels, and the intensity of blue along a measurement channel measured by drawing a line into the blue channel image of the respective channel. Line plot profiles were extracted, plotted in ImageJ and raw data fitted with an error function to model diffusion from a constant concentration source:[7]

$$c(x,t) = c_0 \left[1 - erf \left(\frac{x}{2\sqrt{Dt}} \right) \right],$$

<div align="right">Eq. S1</div>

where c_0 is the initial or constant source concentration, x the position along the measurement channel, t the time and D the diffusion coefficient of the diffusing species (blue dye).

For flow rate testing three independent flow sensors (MFS, Elveflow, France) were added to the zoospore inlet and outlet, and media outlet each and connected with a sensor reader (MSR, Elveflow, France) to record the real-time flow rate of each inlet and outlet using the Elveflow software suite (ESI V3.2.04, Elveflow, France). During the test, DI water was continuously pumped into the platform from the zoospore inlet via the syringe pump at a flow rate of 5 µL/min. Flow circuit modelling was performed using an equivalent circuit model, where a pressure drop ΔP through a straight channel can be summarized as:[8]

$$\Delta P = R_f Q,$$

<div align="right">Eq. S2</div>

where R_f is the fluidic resistance and Q the flow rate. For channels with rectangular cross-section, the fluidic resistance can be expressed as:

$$R_f = \frac{12\eta L}{wh^3 \left(1 - 0.63\frac{h}{w} \right)},$$

<div align="right">Eq. S3</div>

where η is the fluidic viscosity, w and h are the width and height of the channel, respectively. Therefore, when all the microvalves are open, the fluidic layer of the platform could be approximated as shown in Fig. S9(a & b). Each part of the channel was considered as a fluidic resistance and calculated using equation Eq. S3 with the valve section modelled by a straight rectangular channel in first approximation. Then the fluidic resistances of two flow paths, from Zoo.In to Zoo.Out and from Zoo.In to Med.Out, were calculated as 185 and 197 TΩ using an online resistor network solving tool.[9]

For demonstration of the capture and culture function of the platform with integrated normally-closed microvalves, the prepared *A. bisexualis* zoospores were loaded into the devices and the liquid handling structures on the chips used to compartmentalize individual zoospores. To achieve this, the platform was first filled with PYG broth with all membrane valves set to their fully-open state (vacuum pressure applied by OB1 set to -1.0 bar, all MUX switches on). Pre-cultured zoospore solution was then introduced from the zoospore inlet with the syringe pump at a flow rate of 5 µL/min. As a result of this, injected zoospores flowed along the zoospore loading channel and were hydrodynamically captured by the constriction structure in the measurement channels. Once a single zoospore was collected in a trap-site, it was observed using bright-field microscopy and the corresponding microvalve was partially-closed. The latter was achieved by shutting off the switch on the MUX

connected to this microvalve, while pressure from OB1 was kept at -1.0 bar. The same operation was repeated until all the measurement channels had trapped a single zoospore each, after which the zoospore solution was stopped via the external syringe pump. At this point, the system was switched to zoospore maintenance mode, for which the PYG broth was injected into the fluidic layer of platform though the media inlet at a flow rate of 5 µL/min. As opposed to for zoospore loading, the pressure controller OB1 was used for this and continuously supplied media during the entire period of culturing the zoospores on the platform. To conclude trapping and capture, all microvalves were completely closed by applying a positive pressure of 1.0 bar via the OB1 and opening all switches of MUX. All valves were then kept in this state for the entire remaining culture period. For this, all microvalves were operated simultaneously to avoid imposing increasing flow rates and thus shear stresses on zoospores when the microvalves were completely closed one after the other.

The force exerted by germ tubes was determined by a combination of image processing for tracking in ImageJ (V1.51u, FIJI)[10] and subsequent force analysis in MATLAB (V2016a, Mathworks, USA).[11] Image sequences were recorded of hyphae-pillar interaction events and imported into ImageJ, analyzed using the TrackMate plugin[12] and exported in 2D coordinates/time (X,Y, t) format representing the position of the pillar top circle as a function of time. This data was them imported into MATLAB and processed via a custom script. Given a half-hyphal diameter contact height l, both force magnitude f and direction were calculated using an algorithm implemented in MATLAB, which combined pure bending and shear of the imposed force on a cantilever beam:

$$f = \frac{\Delta}{\left(\frac{l^3}{3EI} + \frac{d^2(1+\gamma)l}{4EI}\right) + \frac{l^2}{2EI}(h-l)},$$

Eq. S4

where h is the height of the pillar, d the diameter of the pillar, I is the moment of inertia, and E and γ are Young's modulus and Poisson's ratio for PDMS, respectively.[13,14] Pillar diameters were considered uniform along the height, which was verified by high-magnification optical profilometry (see Fig. S3(d)), thus I could be given by

$$I = \frac{\pi d^4}{64}.$$

Eq. S5

For calibration of force sensing, the Young's modulus of the PDMS devices was determined using bulk PDMS cantilevers. For this, a piezoresistive force sensor setup to measure the Young's modulus was used.[14,15] In addition, values were confirmed using an electromechanical universal test systems (MTS Criterion - model 43) with a 100 N load cell, MTS Testworks 4 software and MTS Videotraction to measure the strain.[16] Finally, force sensing results were exported from Matlab as animated image sequences, force component versus time and total force versus time plots.

Supplementary References:

[1]   X. Li, Z. T. F. Yu, D. Geraldo, S. Weng, N. Alve, W. Dun, A. Kini, K. Patel, R. Shu, F. Zhang, G. Li, Q. Jin and J. Fu, *Review of Scientific Instruments*, 2015, **86**, 075008.

[2]   L. Aoun, P. Weiss, A. Laborde, B. Ducommun, V. Lobjois and C. Vieu, *Lab on a Chip*, 2014, **14**, 2344-2353.

[3]   R. Soffe, A. J. Mach, S. Onal, V. Nock, L. P. Lee and J. T. Nevill, *Small*, 2020, 2002035.

[4]   L. Xu, H. Lee, D. Jetta and K. W. Oh, *Lab on a Chip*, 2015, **15**, 3962-3979.

[5]   S. J. Sowerby, M. F. Broom and G. B. Petersen, *Sensors and Actuators B: Chemical*, 2007, **123**, 325-330.

[6]   R. Vogel, G. Willmott, D. Kozak, G. S. Roberts, W. Anderson, L. Groenewegen, B. Glossop, A. Barnett, A. Turner and M. Trau, *Analytical Chemistry*, 2011, **83**, 3499-3506.

[7]   J. Crank and E. P. J. Crank, *The Mathematics of Diffusion*, Clarendon Press, 1979.

[8]   H. Bruus, *Theoretical Microfluidics*. New York, USA: Oxford University Press, 2008.

[9]   K. Kryukov, "Resistor Network Solver." http://kirr.homeunix.org/electronics/resistor-network-solver/.

[10]   J. Schindelin, I. Arganda-Carreras, E. Frise, V. Kaynig, M. Longair, T. Pietzsch, S. Preibisch, C. Rueden, S. Saalfeld, B. Schmid, J. Y. Tinevez, D. J. White, V. Hartenstein, K. Eliceiri, P. Tomancak, and A. Cardona, *Nature Methods*, 2012, **9**, 676–682.

[11]   Y. Sun, A. Tayagui, A. Garrill and V. Nock, *Journal of Microelectromechanical Systems*, 2018, **27**, 827-835.

[12]   J. Y. Tinevez, N. Perry, J. Schindelin, G. M. Hoopes, G. D. Reynolds, E. Laplantine, S. Y. Bednarek, S. L. Shorte, and K. W. Eliceiri, *Methods*, 2017, **115**, 80–90.

[13]   A. Ghanbari, V. Nock, R. J. Blaikie, J. G. Chase, X. Chen, C. E. Hann and W. Wang, *International Journal of Computer Applications in Technology*, 2010, **39**, 137-144.

[14]   A. Ghanbari, V. Nock, S. Johari, R. J. Blaikie, X. Chen and W. Wang, *Journal of Micromechanics and Microengineering*, 2012, **22**, 095009.

[15]   S. Johari, H. Fazmir, A. F. M. Anuar, M. Z. Zainol, V. Nock, and W. Wang, *IEEE Regional Symposium on Micro and Nanoelectronics (RSM)*, 2015, pp. 1-4.

[16]   A. Tayagui, Y. Sun, D. A. Collings, A. Garrill and V. Nock, *Lab on a Chip*, 2017, **17**, 3643-3653.

Part II: Supplementary figures
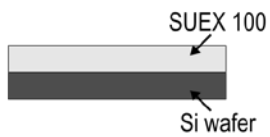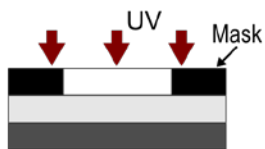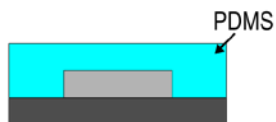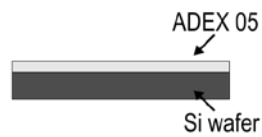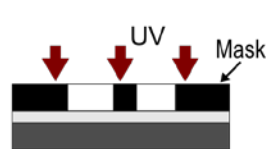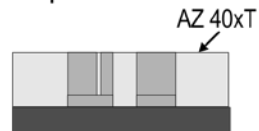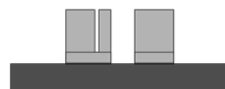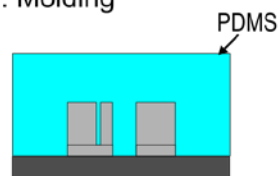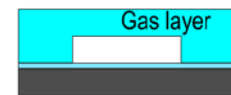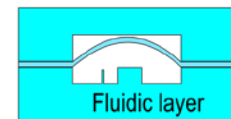
Figure S1: Schematic illustrating device fabrication process. (G1-5) Fabrication of the gas layer mold master using a single dry-film resist layer and replication into PDMS. (F1-7) Fabrication of the fluidic layer mold master using combined positive- and negative-tone resists, and replication into PDMS. (M1) Fabrication of the PDMS membrane by spin-coating. (A1&2) Assembly of the final device using oxygen plasma-bonding and vacuum-assisted layer alignment.
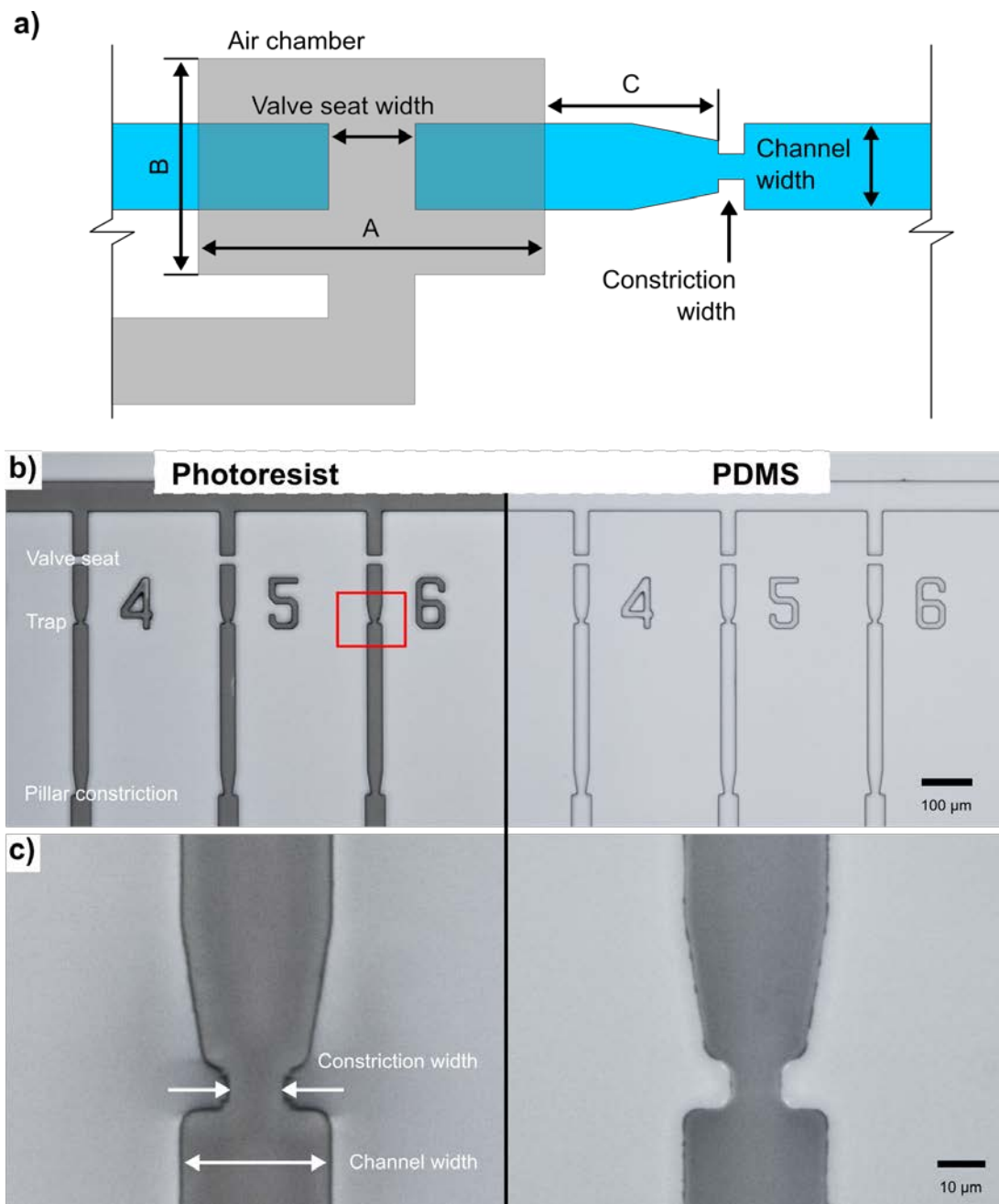
Figure S2: Microvalve and hydrodynamic trap. (a) Schematic of the membrane microvalve and hydrodynamic trap located in the entrance of each measurement channel with parameters air chamber length (*A*), air chamber width (*B*), air chamber-to-trap spacing (*C*), valve seat width, constriction width and channel width shown as defined. (b) Optical micrograph showing three parallel measurement channels in photoresist (*left*) and replicated into PDMS (*right*). Red box indicates the position of the close-up shown in (c). Valve seat, trapping constriction and pillar constriction are visible from top to bottom, in each channel. (c) Optical micrograph close-up of a hydrodynamic trap in photoresist (*left*) and PDMS (*right*).
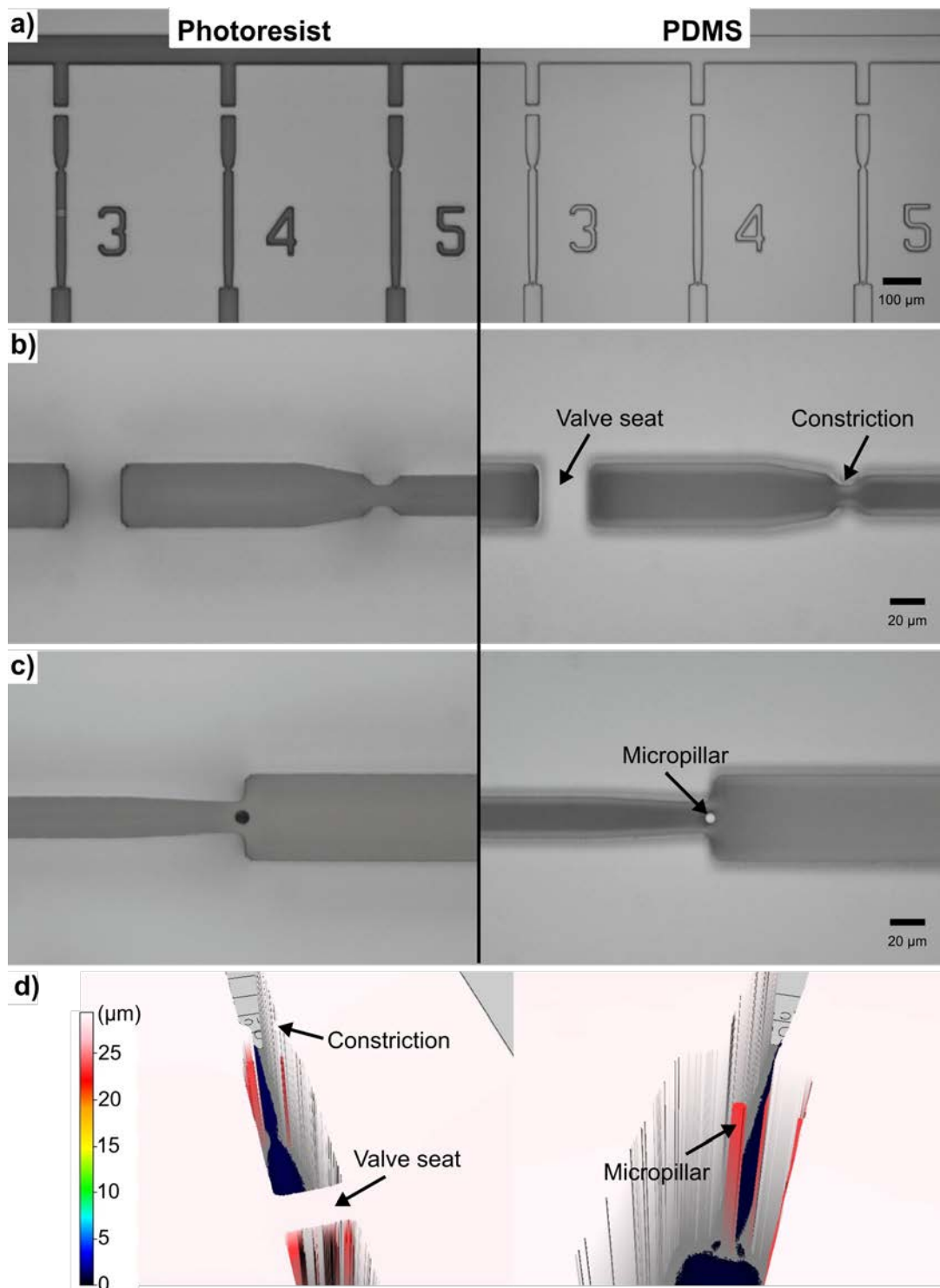
Figure S3: Optical micrographs of fabricated photoresist master and PDMS chip for the fluidic layer. (a) The master wafer and detailed view of the (b) valve seat and constriction structure, and (c) micropillar cavity. Images on the left show the dual-layer resist master, while the corresponding PDMS replicas are shown on the right. (d) Dimensions of the valve seat, trap constriction and high-aspect ratio force measurement micropillar of an example PDMS chip acquired using 3D optical profilometry, As visible from the angle shown on the right, the top of the monolithically-integrated, cylindrical micropillar terminates 5 µm below the channel height.
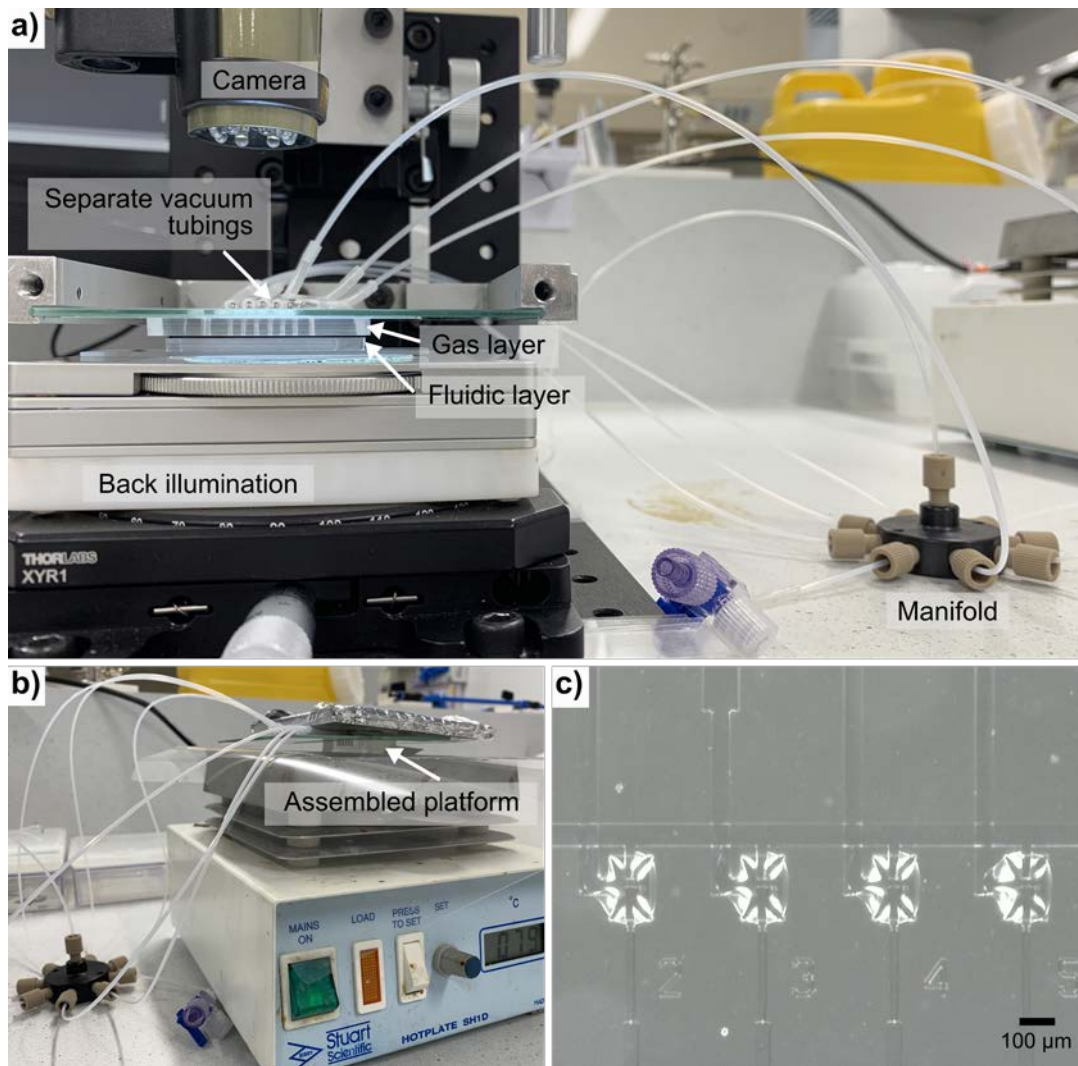
Figure S4: Alignment and bonding processes for the PDMS membrane attached to the gas layer and the fluidic layer. (a) Photograph of the setup adapted for the separated gas inlet configuration. A manual alignment stage was used to align the plasma-activated PDMS layers, while valve membranes were kept retracted using vacuum applied via a gas manifold. (b) Post-bonding bake of the assembled platform on a hotplate with valves retracted. (c) Optical micrograph showing four of the six membrane valves in the retracted state used during device assembly.
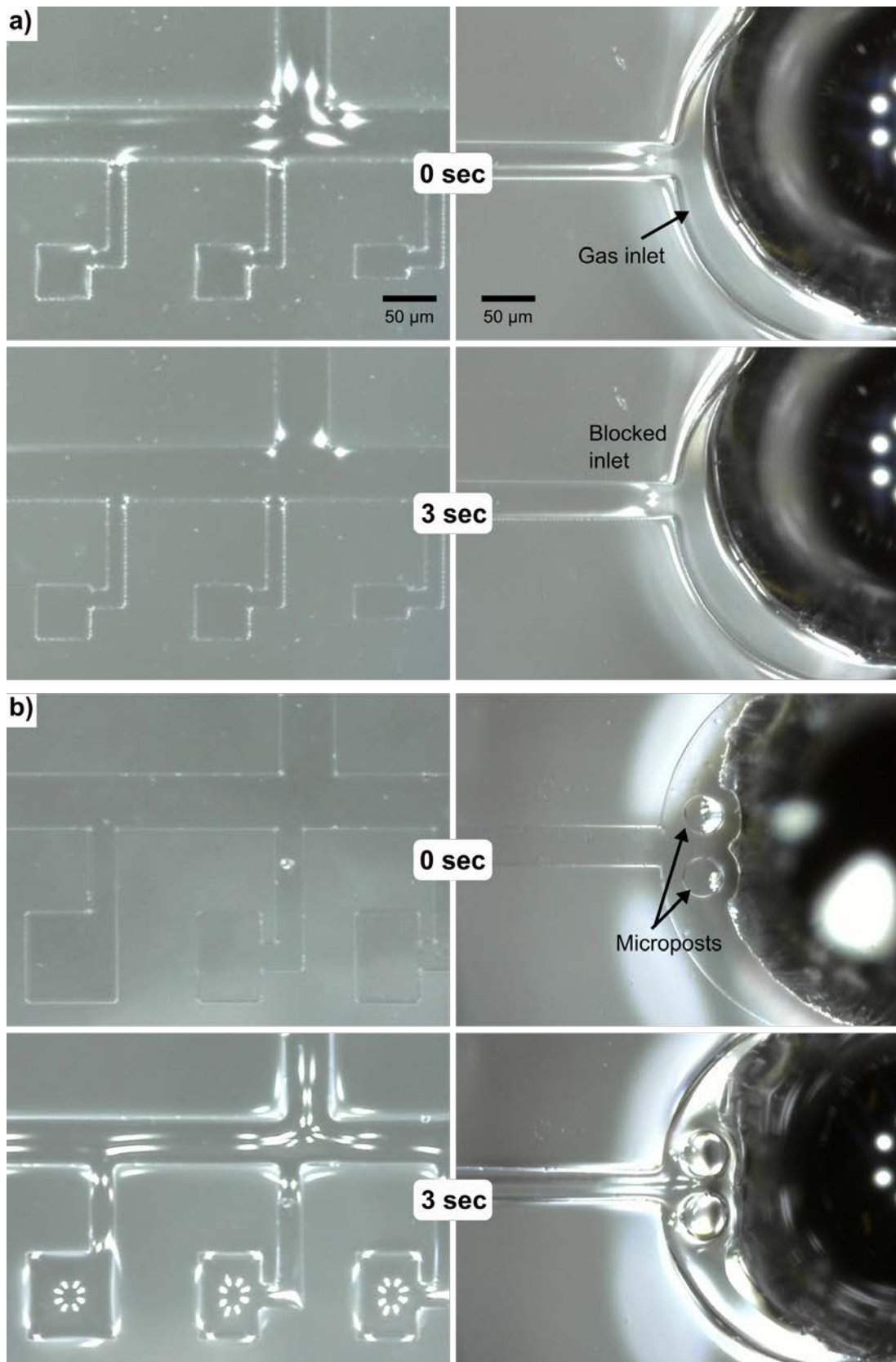
Figure S5: Optical micrographs showing membrane collapse and blockage of the gas layer inlet during PDMS bonding with a vacuum pressure of 0.8 bar applied. (a) Air chambers and their connection channel lost vacuum after vacuum pressure was applied for 3 seconds. This was due to the gas inlet port becoming blocked by the membrane. (b) Vacuum to the air chambers could be sustained after improving the gas inlet port geometry through the addition of microposts into the gas layer design.
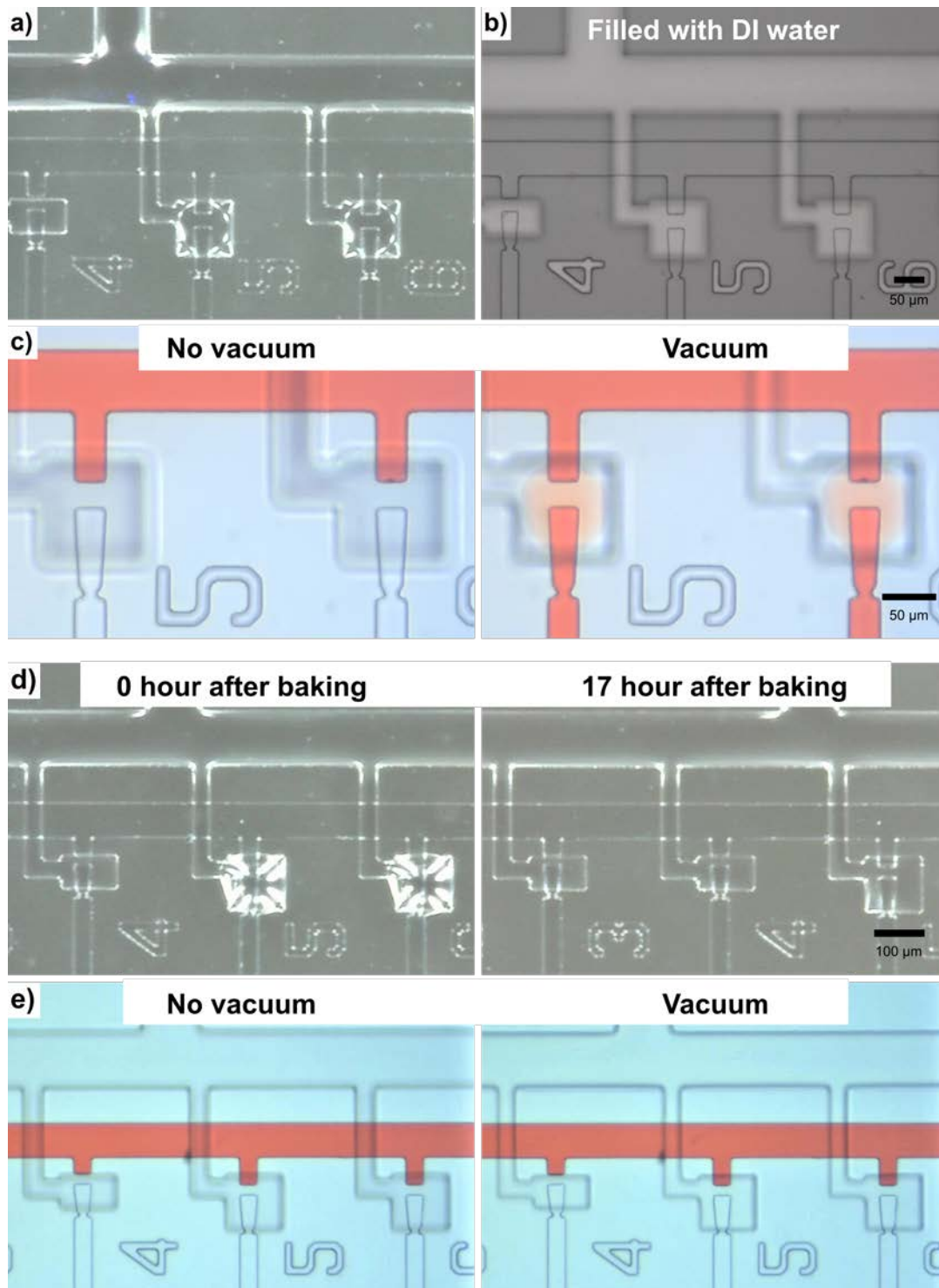
Figure S6: Use of DI water to prevent Valve-sticking. (a) Optical micrograph of the aligned fluidic and gas handling layers during bonding. As can be observed, the valve membranes were kept retracted during this process using vacuum to prevent attachment to the valve seat. (b) Optical micrograph showing the fluidic layer filled with DI water. The device was kept in this state at RT with the membrane relaxed overnight. (c) Flow test showing successful actuation of the valves after assembly with DI. (d) Optical micrographs showing the permanent attachment of valves when assembled dry with the use of vacuum. Valves open directly after end of the bonding bake, but can no longer be actuated 17 hours later, indicating delayed bonding. (e) Flow test showing blocked valves as a result of dry assembly.
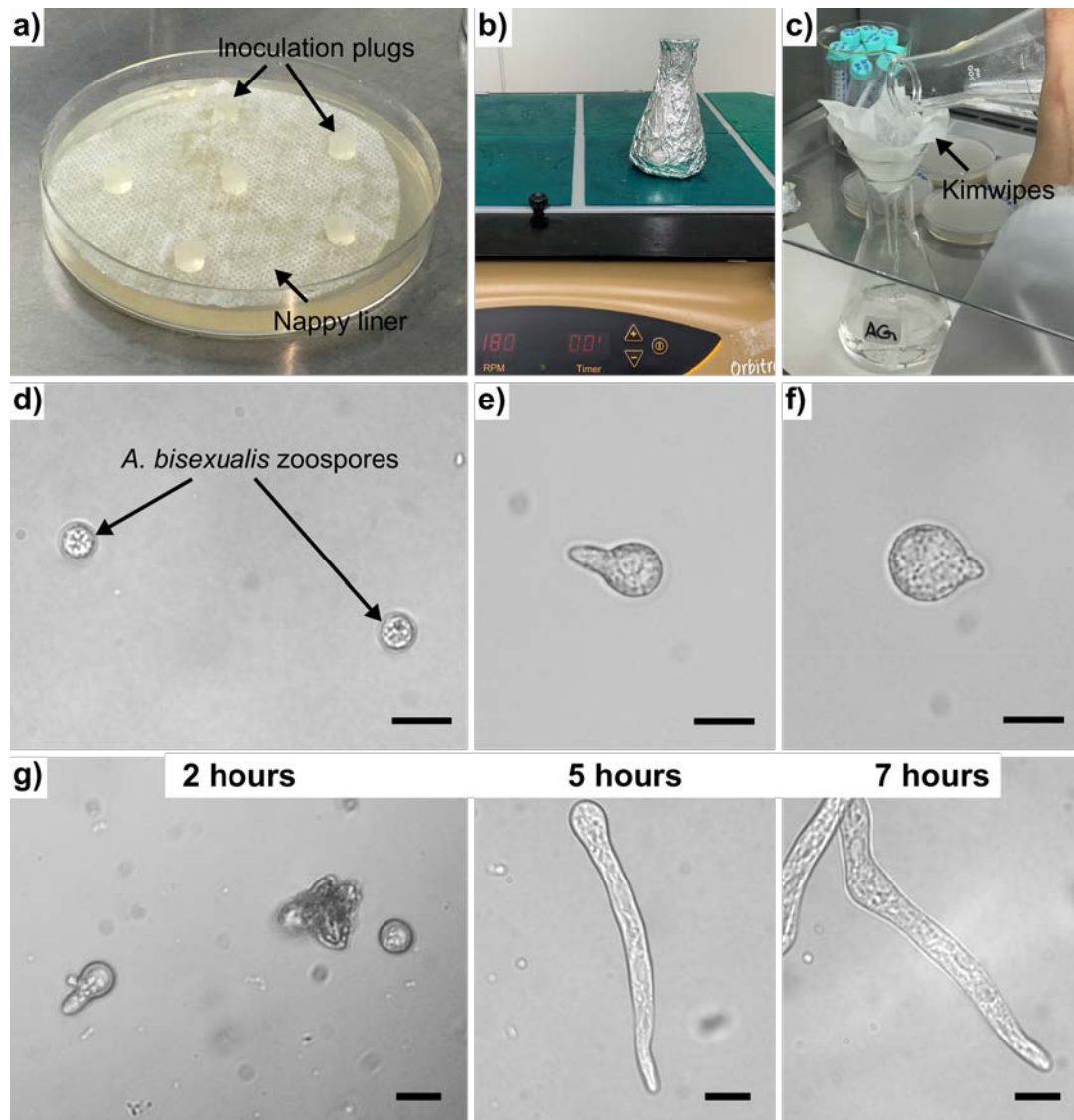
Figure S7: A. bisexualis zoospore induction. (a) Photograph showing six inoculation plugs placed on the PYG agar Petri dish with nappy liner. (b) Photograph of the flask, containing the nappy liner with the growing colony, on an orbital shaker. (c) Photograph showing zoospores being collected in a flask by filtering through Kimwipes. (d) Light micrograph of produced *A. bisexualis* zoospores on a microscope slide. (e & f) Light micrographs of germinating zoospores after 2 hours of being cultured in PYG broth at 26 °C. (g) Light micrographs showing the zoospores germinating and growing in the seeding area of the previous PDMS platform filled with PYG broth after 2, 5, 7 hours, respectively. Scale bars are 20 μm.
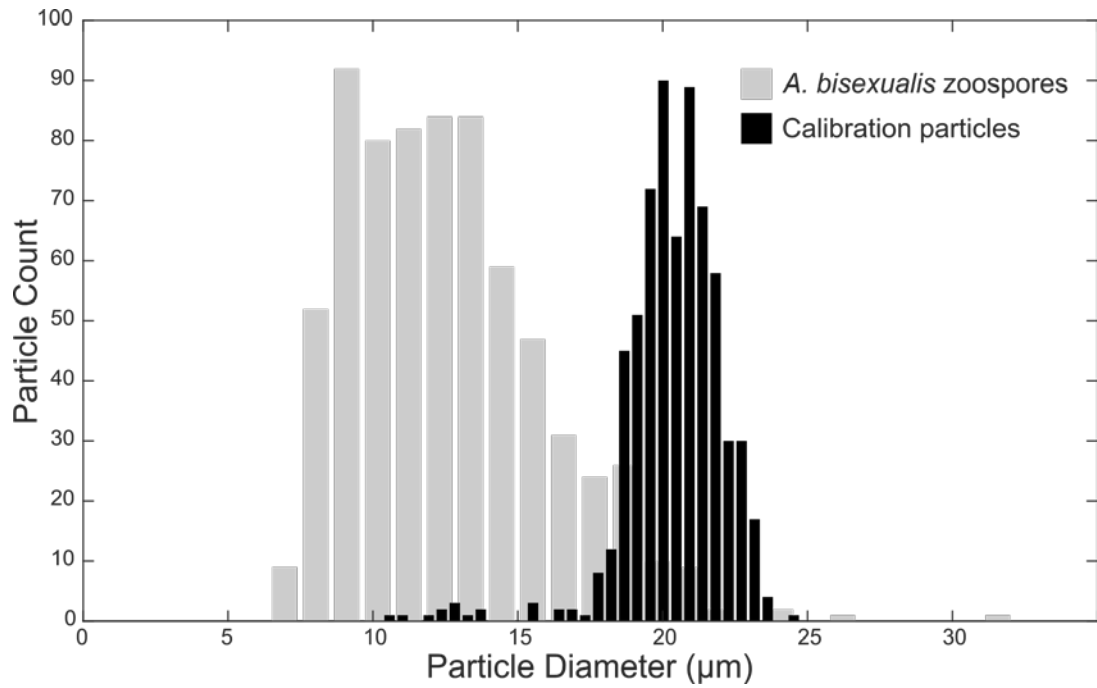
Figure S8: Size distribution of *Achlya bisexualis* zoospores produced through a starvation cycle. Zoospore size (grey) was measured by tuneable-resistive pulse sensing on a qMicro machine and compared to CP20M (mean diameter 20.06 μm) polystyrene calibration particles (black).
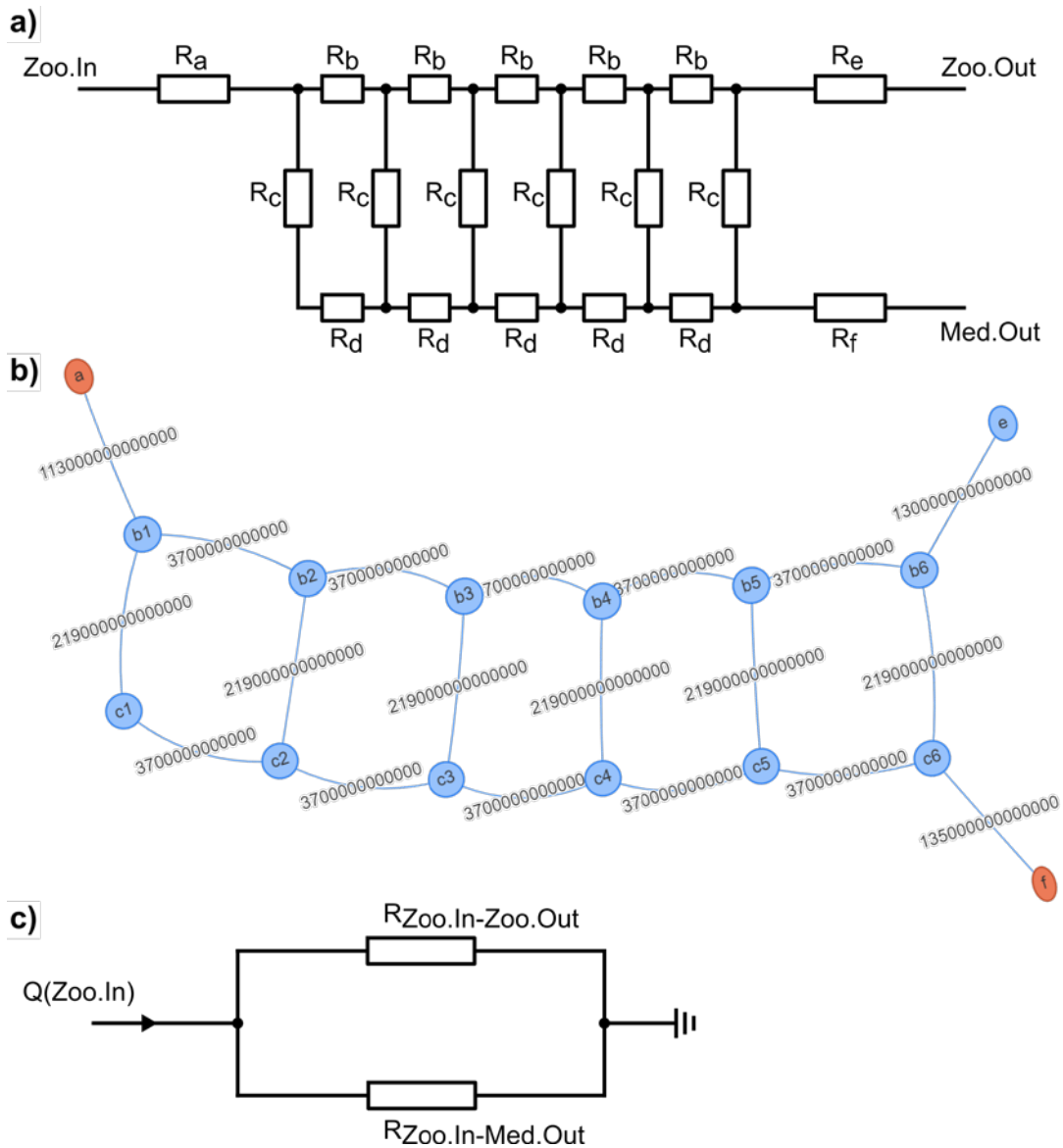
Figure S9: Fluidic resistance estimation for the fluidic layer when all microvalves are open. (a) Schematic showing each part of the channel being considered as a fluidic resistance. (b) Network diagram showing calculated results of fluidic resistances for each part of the channels using equation C.2, as displayed by the online resistor network tool. (c) Schematic showing two flow paths, from Zoo.In to Zoo.Out and from Zoo.In to Med.Out, whose fluidic resistances were calculated using the online tool.
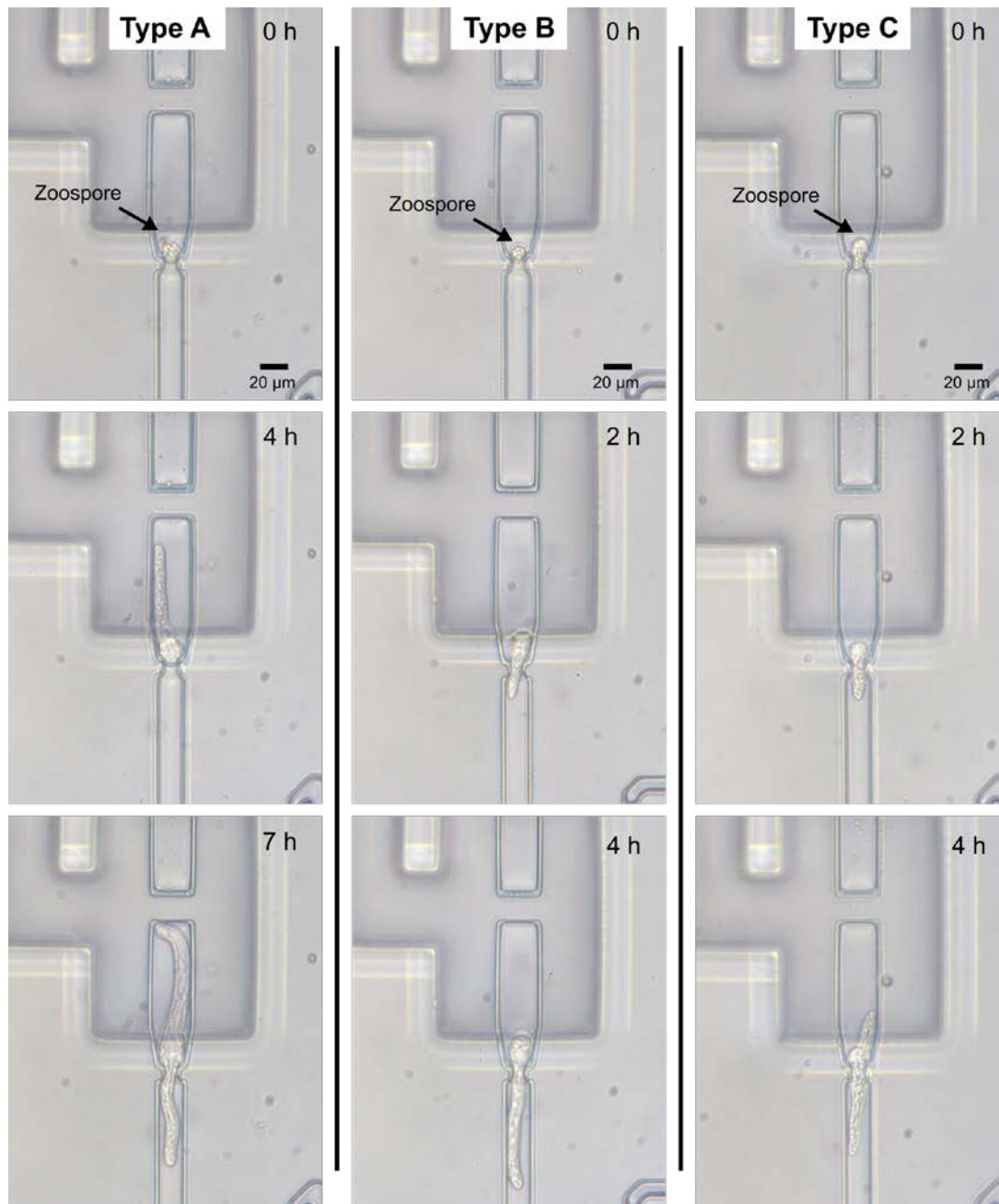
Figure S10: Time-series of optical micrographs showing three specific germination patterns (Type A, B and C) observed for individual *A. bisexualis* zoospores cultured on the platform. For **Type A**, initially, the germlings of the trapped zoospores grew a germ tube towards the valve seat (0 - 4 hours), made contact with the valve seat and stopped growing. Then they branched and put out a second germ tube in the opposite direction, growing through the constriction structure in the measurement channel towards the force sensing micropillar. In **Type B**, the trapped zoospores germinated and grew a germ tube directly through the constriction structure in the measurement channel. **Type C** was the opposite to Type A, with germlings of trapped zoospores firstly growing germ tubes through the constriction structure (0 - 2 hour). However, at some point, germlings branched and put out a new germ tube in the opposite direction towards the valve seat. The new germ tubes stopped growing after around 2 hours, while the former one kept growing and ultimately hit and passed the micropillar (4 hours).
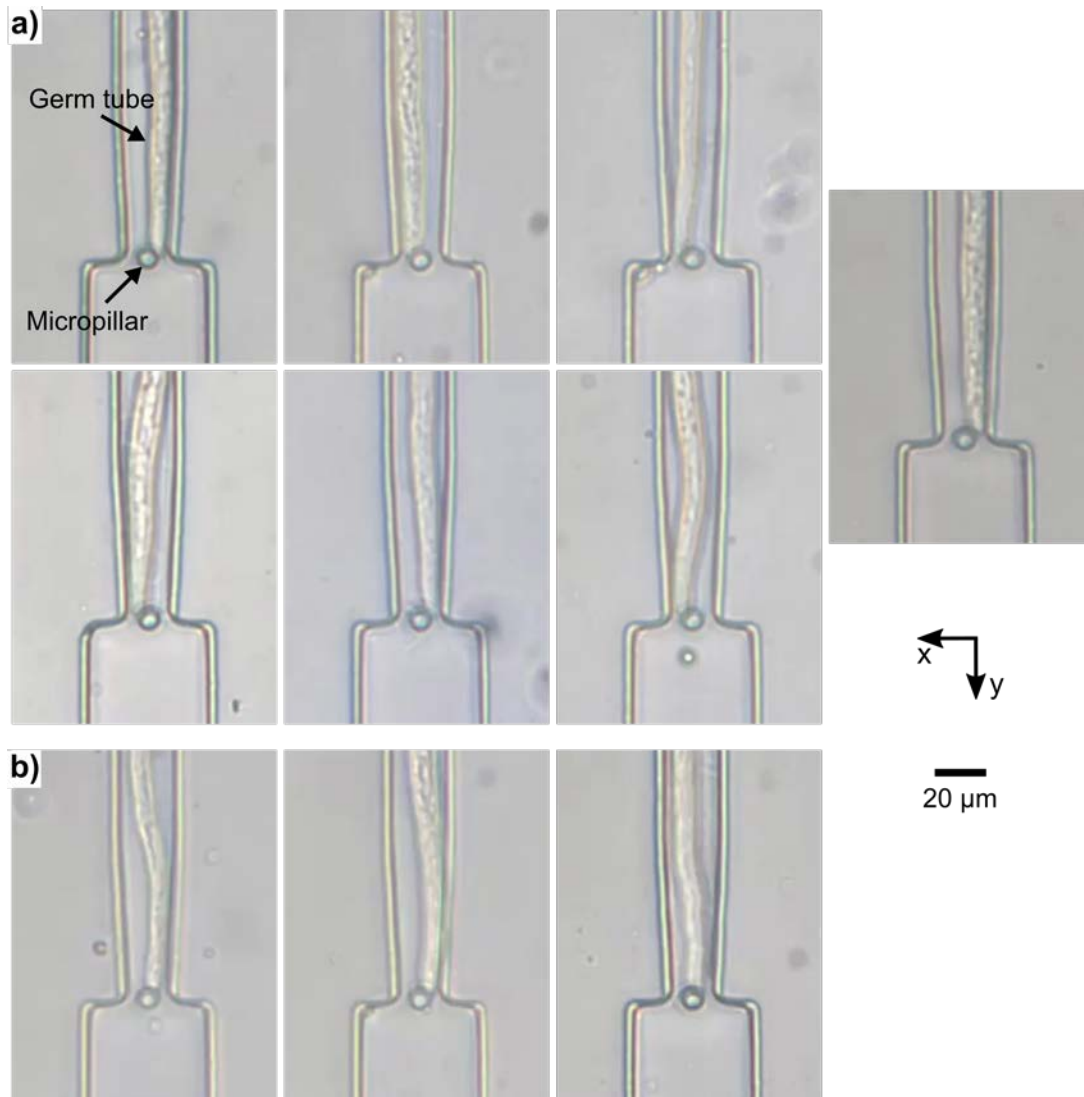
Figure S11: Optical micrographs showing all the 10 cases where germ tubes originating from single *A. bisexualis* zoospores hit the force sensing micropillars. (a) 7 lateral hit and (b) 3 direct hit cases out of the total 10 recorded impact cases.

Part III: Supplementary movies

Movie V1: "Microparticle Valving" contains the video results of microvalve opening tests with 20 μm polystyrene microparticles suspended in dyed water shown in Fig. 3. Normally-off PDMS membrane microvalves of various air chamber widths and lengths were tested to determine the optimum dimensions for particle transfer to the hydrodynamic traps.

Movie V2: "Valve Closure Test" contains the video results for the flow test to establish valve sealing and diffusion-based exchange of liquid in measurement channels described in Fig. 4.

Movie V3: "Zoospore Trapping" contains the video results of hydrodynamic trapping and compartmentalization of *A. bisexualis* zoospores shown in Fig. 6. Normally-off PDMS membrane microvalves are closed after trapping via application of compressed gas to compartmentalize zoospores into measurement channels.

Movie V4: "Germ Tube Force Sensing" contains the video results of four example germ tubes deflecting the force measurement pillars. For each case, the full germ tube from the trap to the pillar location is shown, as well as a close-up of the pillar deflection with force vector overlaid, indicating magnitude and direction of the force imparted by the germ tube tip. Events were recorded at 0.5 fps and are played back at 8x the normal speed.